Pure appl. geophys. 166 (2009) 1629–1648
0033–4553/09/101629–20
DOI 10.1007/s00024-009-0512-3

Pure and Applied Geophysics

Effects of Off-fault Damage on Earthquake Rupture Propagation: Experimental Studies

Charles G. Sammis,[1] Ares J. Rosakis,[2] and Harsha S. Bhat[1,2]

Abstract—We review the results of a recent series of papers in which the interaction between a dynamic mode II fracture on a fault plane and off-fault damage has been studied using high-speed photography. In these experiments, fracture damage was created in photoelastic Homalite plates by thermal shock in liquid nitrogen and rupture velocities were measured by imaging fringes at the tips. In this paper we review these experiments and discuss how they might be scaled from lab to field using a recent theoretical model for dynamic rupture propagation. Three experimental configurations were investigated: An interface between two damaged Homalite plates, an interface between damaged and undamaged Homalite plates, and the interface between damaged Homalite and undamaged polycarbonate plates. In each case, the velocity was compared with that on a fault between the equivalent undamaged plates at the same load. Ruptures on the interface between two damaged Homalite plates travel at sub-Rayleigh velocities indicating that sliding on off-fault fractures dissipates energy, even though no new damage is created. Propagation on the interface between damaged and undamaged Homalite is asymmetric. Ruptures propagating in the direction for which the compressional lobe of their crack-tip stress field is in the damage (which we term the 'C' direction) are unaffected by the damage. In the opposite 'T' direction, the rupture velocity is significantly slower than the velocity in undamaged plates at the same load. Specifically, transitions to supershear observed using undamaged plates are not observed in the 'T' direction. Propagation on the interface between damaged Homalite and undamaged polycarbonate exhibits the same asymmetry, even though the elastically "favored" '+' direction coincides with the 'T' direction in this case. The scaling properties of the interaction between the crack-tip field and pre-existing off-fault damage (i.e., no new damage is created) are explored using an analytic model for a nonsingular slip-weakening shear slip-pulse and verified using the velocity history of a slip pulse measured in the laboratory and a direct laboratory measurement of the interaction range using damage zones of various widths adjacent to the fault.

Key words: dynamic rupture, fracture damage, supershear rupture, asymmetric propagation, fault zone, slip pulse.

1. Introduction

Although earthquakes are commonly modeled as frictional instabilities on planar faults, real faults, many of which have been exhumed from seismogenic depths, have a more complex structure shown schematically in Figure 1. Most slip occurs in a highly

[1] Department of Earth Sciences, University of Southern California, Los Angeles, CA 90089-0740, U.S.A.
[2] Graduate Aeronautical Laboratories, 1200 E. California Blvd., Pasadena, CA 91125, U.S.A.

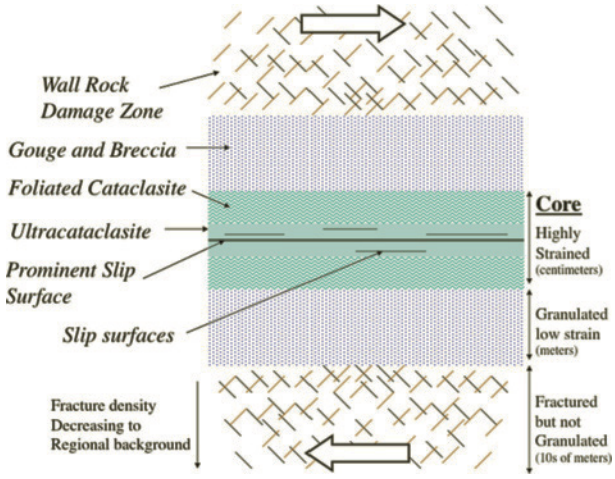

Figure 1
Schematic cross section of an idealized fault at seismogenic depth. The nested layered structure is described in the text. The widths of the layers vary from fault to fault, and the structure is often less symmetric than shown here.

sheared "core," typically a few centimeters thick, and composed of extremely fine-grained granulated rock (known as cataclasite) which is commonly altered to clay mineralogy, particularly at shallow depths. Slip within the core is often localized onto principal slip surfaces a few mm thick and composed of still finer-grained ultracataclasites. The core is bordered by layers of coarser granulated rock commonly termed gouge or fault breccia. These layers are typically meters thick and appear to have accommodated little or no shear strain. For some large displacement strike-slip faults, "pulverized rocks" in which individual grains are shattered but the rock fabric is undisturbed have been observed to distances of 100–300 meters from the fault plane in formations that were at or near the surface during faulting (Dor *et al.*, 2006). The granular layers are bordered by highly fractured (but not granulated) wall rock within which the fracture density decreases to the regional background value over a distance of a few hundred meters. More detailed descriptions of fault zone structure, deviations from the ideal symmetry in Figure 1, and discussions as to how it might have formed are given by Ben-Zion and Sammis (2003) and Biegel and Sammis (2004).

The focus of this paper is on how fault zone structure affects earthquake rupture propagation, with special emphasis on a series of recent laboratory measurements of rupture velocity on faults in damaged photoelastic plates by Biegel *et al.* (2008, 2009) and Bhat *et al.* (2009). Biegel *et al.* (2008) observed a reduction in rupture velocity caused by a symmetric distribution of damage about a premachined fault, and measured the spatial extent of the interaction between the rupture tip and the off-fault damage. Biegel *et al.* (2009) and Bhat *et al.* (2009) studied propagation asymmetries caused by slip on the interface between damaged and undamaged materials, as would be the case if

an earthquake rupture propagated along one side of a fault zone. A key question here is: How wide does the fault zone have to be in order to affect rupture propagation? We address this question at the end of the paper by using a recent dynamic slip pulse model (RICE *et al*., 2005) as guidance in scaling observations in the laboratory to natural earthquakes.

Consider first the case of symmetric off-fault damage with no material contrast. A first-order effect of fracture damage on rupture propagation is to lower the elastic stiffness of the material. By reducing the shear-wave speed c_S, the effect on rupture velocity is to lower the limiting Rayleigh speed, which is 0.92 c_S for Mode II ruptures. However, BIEGEL *et al*. (2008) found that damage reduced the rupture velocity below that expected, based solely on the lower shear-wave speed. They ascribed this additional reduction to a further dynamic reduction in modulus and to anelastic losses associated with frictional slip on the myriad of small off-fault fractures that comprise the damage.

BIEGEL *et al*. (2009) and BHAT *et al*. (2009) extended these measurements to ruptures that propagate on the interface between damaged and undamaged materials. In these experiments, the off-fault damage produced additional asymmetries in the propagation of ruptures beyond those expected from the associated contrast in elastic stiffness. Propagation asymmetries ascribed to the damage were observed to be stronger than those due to elastic contrasts.

2. *Experimental Apparatus*

All experiments described here used the apparatus shown in Figure 2. Square plates of the photoelastic polymers Homalite and polycarbonate were prepared with a premachined fault at an angle α to the edge as in Figure 3. The plates were loaded with a uniaxial stress P and a bilateral rupture was nucleated using a high-voltage pulse to explode a wire in a small hole that crossed the center of the fault plane. The explosion reduced the normal stress on an $\sim$1-cm long patch of the fault plane, allowing shear slip that nucleated the rupture. The voltage pulse was also used to trigger a pair of high-speed digital cameras that recorded a series of images of the shear stress field revealed as fringes in polarized laser light.

The upper panel in Figure 4 shows four frames taken at the times indicated during one of the Homalite experiments. Fringes associated with stress concentration at the rupture fronts and the S wave generated by the nucleation event can be identified. The lower panel in Figure 4 shows the corresponding instantaneous velocity as a function of time. Instantaneous velocity was found by differentiating an interpolated cubic spline fit to the displacements using a MATLAB® utility (BIEGEL *et al*., 2009; BHAT *et al*., 2009). Note that propagation is symmetric and both rupture tips accelerate to the limiting (Rayleigh) rupture velocity $c_R = 0.92c_S$ for mode II propagation and then transition to supershear velocities approaching the P-wave speed (note, $c_P/c_S = 2.1$ for Homalite).

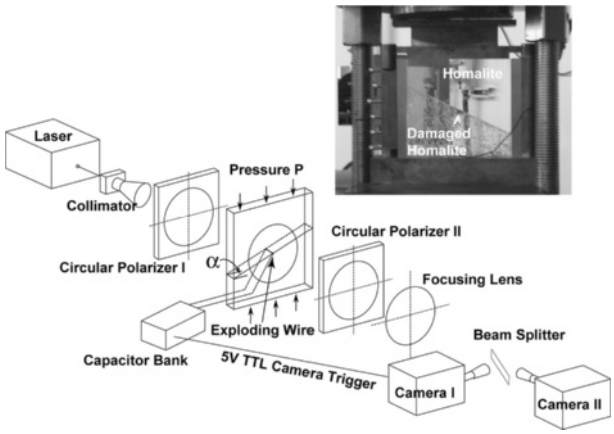

Figure 2
Schematic diagram of apparatus used to take a series of high-speed photographs of dynamic ruptures on premachined faults in photoelastic Homalite and polycarbonate plates. The inset shows a sample in the loading frame used to apply uniaxial stress *P*.

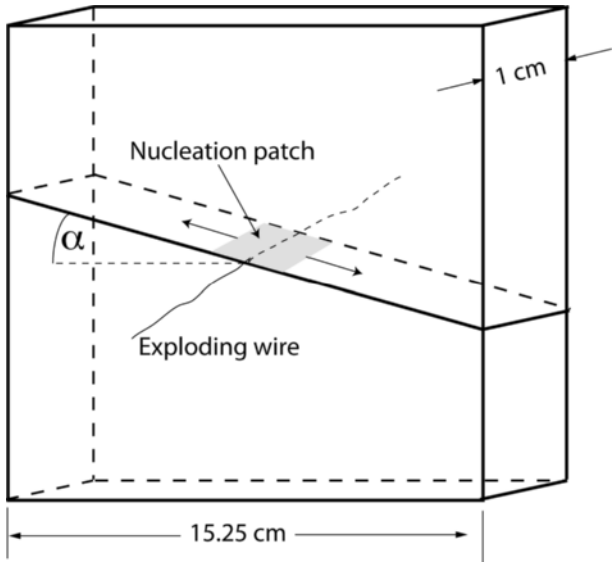

Figure 3
Sample geometry showing premachined fault at angle α. The exploding wire is used to create a patch of low effective normal stress that nucleates a bilateral rupture at the center of the fault plane.

3. *Effect of Symmetric Off-Fault Damage on Rupture Velocity*

BIEGEL *et al*. (2008) introduced fracture damage into Homalite plates by using a razor knife to score a mesh of scratches on both sides of the plate spaced about 2 mm apart and

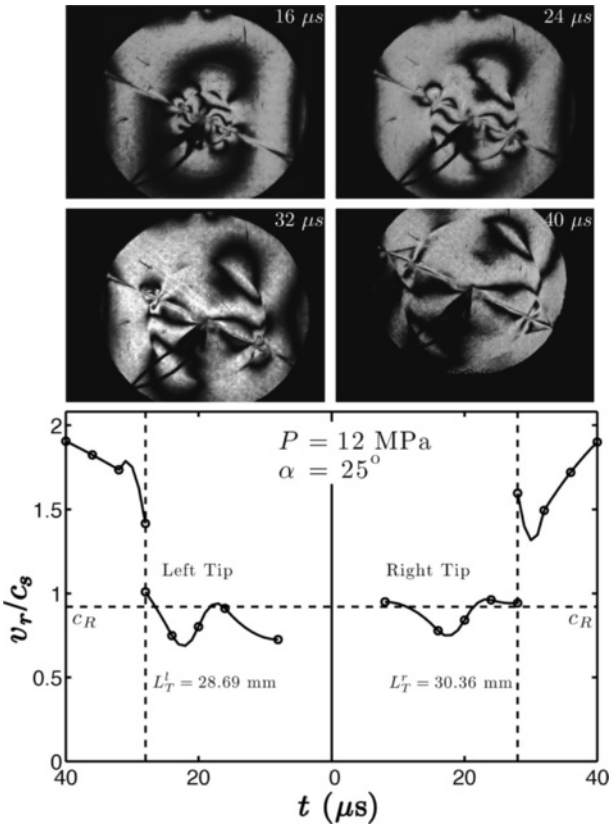

Figure 4

Dynamic rupture on the interface between two Homalite plates. The upper four panels show frames from the sequence of high-speed photographs taken at the times indicated. Note the butterfly-like stress concentrations at the rupture front in the frame taken at 24 μs. The shear stress concentration associated with the S wave generated at nucleation is most evident at 2 and 7 o'clock in the frames taken at 32 and 40 μs. The Mach cone produced by supershear propagation is most evident in the frame taken at 40 μs. The lower panel shows the instantaneous velocity of the rupture tips as a function of time. Note that propagation is symmetric. Both tips propagate near the Rayleigh velocity $c_R = 0.92c_S$ for about 29 μs before transitioning to supershear velocities approaching c_P.

oriented at +/− 45° to the loading axis, followed by immersion in liquid nitrogen for 45 seconds. The thermal shock produced a network of fractures with a mean spacing of about 1 cm as shown in Figure 5. Travel-time curves measured for both rupture fronts and for the S-wave are plotted in Figure 6 where they are compared with those for the undamaged Homalite. Note that rupture velocity and S-wave speed in the damaged plates are lower than those in the undamaged plates. More importantly, the ratio v_r/c_S is significantly smaller in the damaged material where it is less that the Rayleigh speed ($v_r < 0.92c_S^{DH}$, where c_S^{DH} is the shear speed in damaged Homalite). The implication is that the rupture velocity is further reduced by anelastic loss due to frictional sliding on the

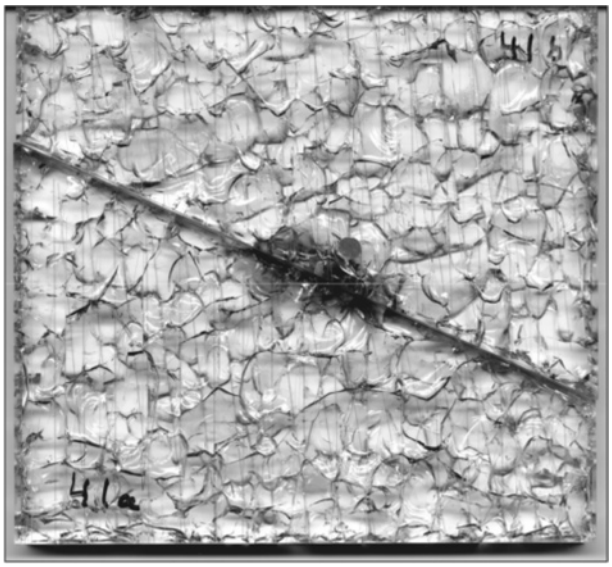

Figure 5
Fracture-damaged sample produced by first scoring both sides of the Homalite plates with a razor knife and then submersing in liquid nitrogen for 45 seconds. The center of the fault plane has been darkened by the explosion that nucleated rupture.

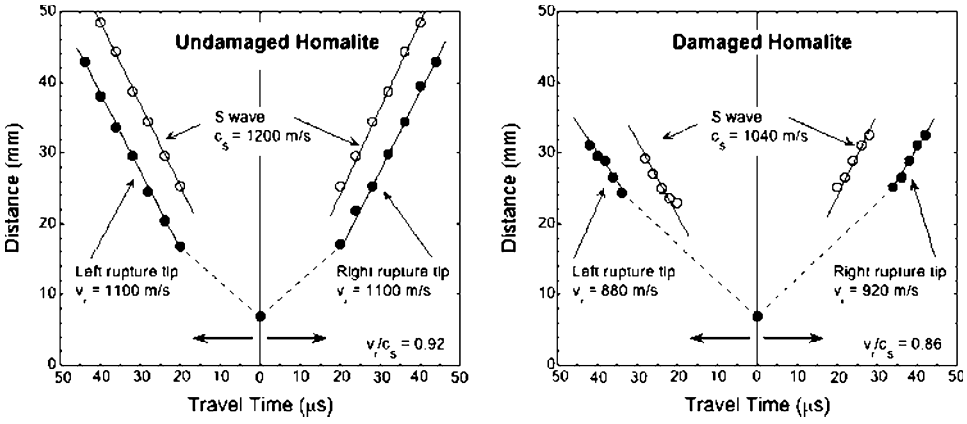

Figure 6
Travel time curves for a rupture propagating on the interface between two undamaged Homalite plates on the left, and between two fracture-damaged Homalite plates on the right. S-wave travel times are also plotted. $P = 12$ MPa and $\alpha = 25°$ in both tests. Note that rupture in undamaged Homalite did not transition to supershear as in Figure 4. Since the load was the same, the difference was probably due to the slightly rougher sliding surface in this case (see ROSAKIS *et al.*, 2008).

off-fault fractures. No additional off-fault damage was created by the rupture in these experiments.

4. *Effect of Asymmetric Off-Fault Damage on Rupture Velocity and Directionality*

BIEGEL *et al*. (2009) used the apparatus in Figure 2 to measure the velocity of ruptures on the interface between damaged and undamaged Homalite. As illustrated in Figure 7, the symmetry in these experiments is broken in two ways: elastically and anelastically. The elastic asymmetry is caused by the change in elastic modulus across the fault plane, and results in different propagation velocities in the '+' direction (the direction in which the lower velocity damaged Homalite moves) and in the opposite '−' direction. The physical cause of this elastic asymmetry is tension across the fault plane at the tip of the rupture propagating in the '+' direction (WEERTMAN, 1980; HARRIS and DAY, 1997; COCHARD and RICE, 2000; RANJITH and RICE, 2001; BEN-ZION, 2001; XIA *et al*., 2005b; SHI and BEN-ZION, 2006; RUBIN and AMPUERO, 2007; AMPUERO and BEN-ZION, 2008).

Prior experimental studies in such elastic bi-materials by XIA *et al*. (2005b) found that ruptures in the '+' direction propagate at the generalized Rayleigh wave speed while those in the opposite '−' direction transition to super shear velocities that approach $P_{\text{slow}} \equiv c_P^{\text{slow}}$, the P-wave speed in the material having slower wave speeds. Theoretical studies have shown that, depending on the friction law, loading and nucleation conditions, a transition to supershear propagation is also possible in the '+' direction with velocity approaching $P_{\text{fast}} \equiv c_P^{\text{fast}}$, the P-wave speed in the material having faster wave

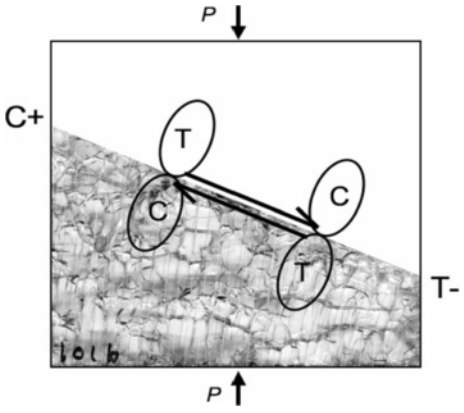

Figure 7
Asymmetries in an undamaged Homalite plate in contact with a damaged Homalite plate. Since the damaged Homalite is slightly less stiff than the undamaged Homalite, the '+' direction of propagation is to the left, which by convention is the direction of motion of the less stiff material. The anelastic asymmetry is denoted by the 'C' propagation direction for which the compressional lobe of the crack-tip stress concentration travels through the damage and the 'T' direction for which the crack tip places the damage in tension.

speeds (COCHARD and RICE, 2000; RANJITH and RICE, 2001, SHI and BEN-ZION, 2006). BHAT *et al*. (2009) observed simultaneous supershear propagation in the '+' direction at P_{fast} and in the '−' direction at P_{slow}. SHI and BEN-ZION (2006) observed such simultaneous supershear propagation velocities in simulations with a nucleation procedure that imposed supershear rupture in the nucleation zone.

We hypothesize that the anelastic asymmetry arises because one fracture tip has the compressive lobe of its stress concentration in the damage (which we term the 'C' direction) while the other tip has its tensile lobe in the damage (which we term the 'T' direction). For example, in Figure 7 the rupture tip moving to the left is labeled 'C+' because it is moving in the '+' direction (the direction of motion of the more compliant damaged Homalite) and 'C' because the compressive stress concentration lies in the damage. Following this convention, the tip moving to the right is labeled 'T−'. We propose that the physical cause of the anelastic asymmetry is that tension in the 'T' direction enhances sliding on the off-fault cracks that comprise the damage while compression in the 'C' direction suppresses such sliding. This asymmetry is evident in Figure 8, which shows the velocities measured by BIEGEL *et al*. (2009) for a rupture on the interface between damaged and undamaged Homalite. Note that the rupture running in the 'C+' direction moves at P_{fast}, the expected velocity in the '+' direction for an elastic bi-material. Off-fault damage appears to have little additional effect in the 'C' direction, presumably because sliding is suppressed by the crack-tip compression. However, note that the rupture in the 'T−'direction stops. The interpretation is that tension enables energy dissipation by frictional sliding in the off-fault damage near the crack tip that completely suppresses propagation. The full set of rupture velocities measured by BIEGEL *et al*. (2009) on interfaces between Homalite and damaged Homalite is summarized in Figure 9 where they are compared with measurements at the same loads for the undamaged Homalite system. Note that ruptures in the 'C+' direction are only slightly affected by the damage while those in the 'T−' direction are severely slowed or even stopped, especially at the highest loads.

The rupture velocity in the all-damaged Homalite sample at $P = 12$ MPa (Figs. 5 and 6) is also plotted in Figure 9 where it is seen to be the same as the velocity in the 'T−' direction on the interface between Homalite and damaged Homalite (also at 12 MPa). This is the expected result based on our hypothesis that the compressive side of the rupture does not see the damage.

BHAT *et al*. (2009) extended this work by measuring rupture velocities on the interface between damaged Homalite and undamaged polycarbonate (which has a slightly lower shear-wave speed than does damaged Homalite). However, for comparison, they first measured the velocity of ruptures on the interface between undamaged Homalite and undamaged polycarbonate. The results of a typical experiment are shown in Figure 10 where four frames of the high-speed sequence (taken at the times indicated) are shown in the upper panel and the velocities are shown in the lower panel. Note that left rupture propagating in the '+' direction transitions to supershear velocities approaching P_{fast} while the right rupture propagating in the '−' direction approaches P_{slow}. This bimaterial

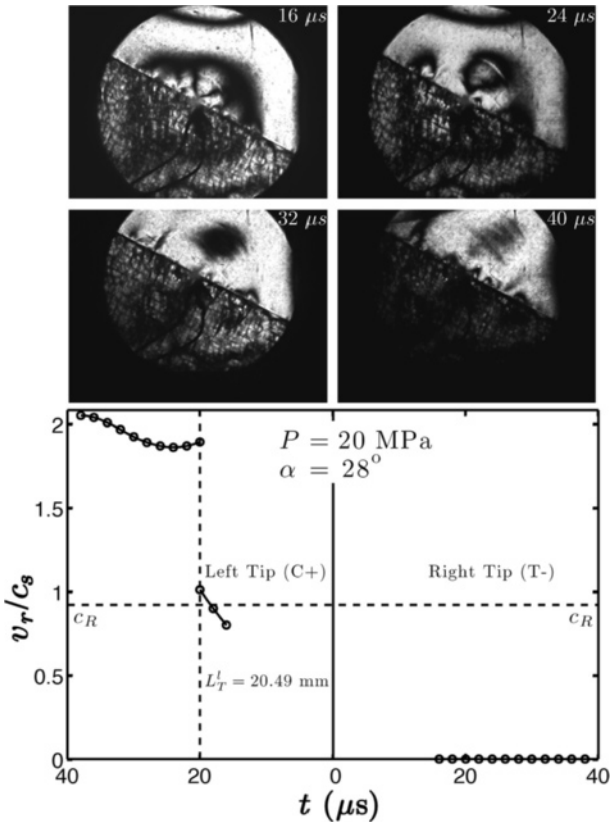

Figure 8

Dynamic rupture on the interface between damaged and undamaged Homalite plates. The upper four panels show frames at the times indicated selected from the sequence of high-speed photographs. The lower panel shows the instantaneous velocity of the rupture tips as a function of time. Note that the left tip propagating in the 'C+' direction transitions to supershear as in Figure 4 but that rupture propagation in the 'T−' direction is completely suppressed, presumably by energy loss on the off-fault damage activated by the tensile lobe of the stress field.

system was explored in more detail by Xia *et al*. (2005b), although they never observed supershear in both directions as in Figure 10, probably because the propagation distance to the supershear transition in their experiments was longer than the radius of the observable circle due to their rougher sliding surfaces (see Rosakis *et al*., 2008 for a discussion of the supershear transition length).

The elastic and anelastic asymmetries that arise when damaged Homalite is in sliding contact with undamaged polycarbonate are illustrated in Figure 11. Since undamaged polycarbonate has a lower elastic stiffness than does damaged Homalite, propagation directions in these experiments are 'T+' to the left and 'C−' to the right (see Table 1 for a summary of the elastic properties of Homalite, damaged Homalite, and polycarbonate).

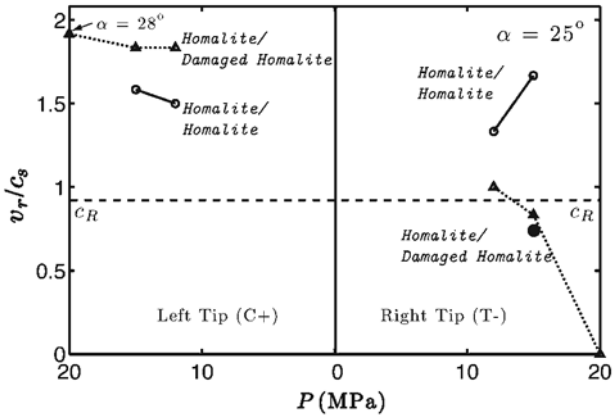

Figure 9
Summary of experimental results comparing rupture velocity in damaged bimaterial samples with those in undamaged Homalite plates. Note that the off-fault damage has little effect on ruptures traveling in the 'C+' direction but a major effect on those propagating in the 'T−' direction. Bimaterial ruptures which have the tensile lobe in the damage did not transition to supershear and, at large uniaxial loads, did not propagate at all. The solid circle is for damaged Homalite/damaged Homalite at $P = 12$ MPa from Figure 6 (from BIEGEL *et al.*, 2009).

Figure 12 shows the rupture velocities on the interface between damaged Homalite and polycarbonate for $P = 15$ MPa and $\alpha = 25°$. Note that in the 'T+' direction the rupture velocity approaches the generalized Rayleigh speed while in the 'C−' direction it slowly increases above the generalized Rayleigh speed, possibly toward P_{slow}, the P-wave speed in polycarbonate. The full set of rupture velocities measured by BHAT *et al.* (2009) on interfaces between damaged Homalite and polycarbonate is summarized in Figure 13 where they are compared with the measured velocity of ruptures at the same loads on the interface between undamaged Homalite and polycarbonate. As in the previous case of Homalite in contact with damaged Homalite, ruptures in the 'C' direction are only slightly affected by the damage. Like rupture velocities in the undamaged system, they appear to be increasing toward P_{slow}, but only at higher loads. Ruptures in the 'T' direction are more severely affected by the damage. The transition to supershear, which takes place in the undamaged system, is suppressed in the damaged system where ruptures propagated at the generalized Rayleigh speed for applied loads up to 15 MPa.

5. Scaling Laboratory Studies to Natural Fault Zones

Since the anelastic propagation asymmetry is caused by the interaction of the crack tip stress concentration with the off-fault damage, it is important to know the spatial extent of this crack tip field and how it scales from the ruptures in photoelastic polymer plates in the laboratory to earthquakes on natural faults in rock. The answer can be found

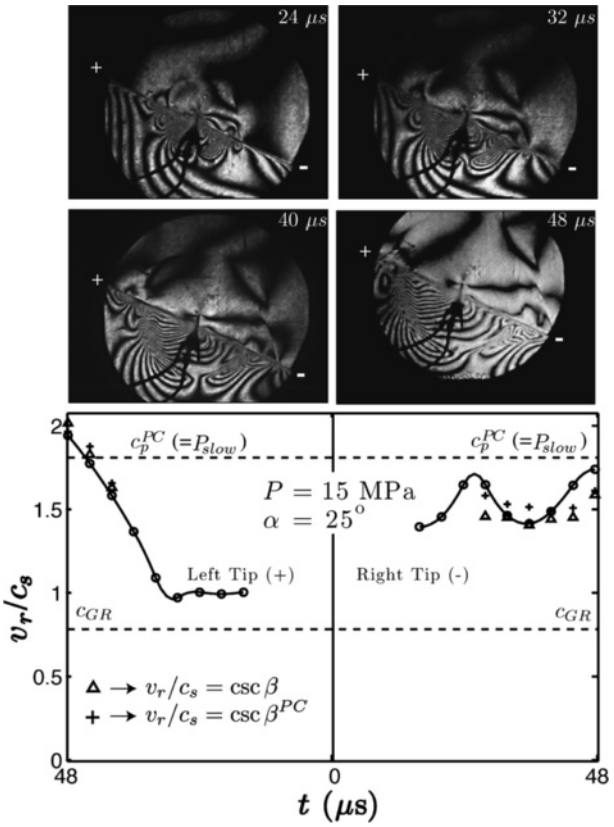

Figure 10

Dynamic rupture on the interface between undamaged Homalite and undamaged polycarbonate plates. The upper four panels show frames at the times indicated selected from the sequence of high-speed photographs. The lower panel shows the instantaneous velocity of the rupture tips as a function of time. Note that the left tip propagating in the '+' direction transitions to supershear velocities approaching P_{fast}. The right tip propagating in the '−' direction also transitions to supershear velocities approaching P_{slow}. The + and Δ symbols indicate propagation velocities determined for the angle β of the Mach cone in Homalite and in polycarbonate respectively (from BHAT *et al*., 2009).

using an analytic model for a dynamic slip pulse developed by RICE *et al*. (2005) (hereafter referred to as RSP). The geometry and parameters of the model are illustrated in Figure 14. The spatial extent of the off-fault stress field depends on four nondimensional parameters: the ratio of components of the prestress $\sigma^o_{xx}/\sigma^o_{yy}$, the ratio of the rupture velocity to the shear-wave speed v_r/c_S, the ratio of the residual to peak stress τ_r/τ_p, and the length of the slip-weakening zone relative to the length of the slip pulse *R/L*. As illustrated in Figure 15, RSP found that the spatial extent of the stress concentration is larger for smaller values of $\sigma^o_{xx}/\sigma^o_{yy}$ (when the stress vector makes a

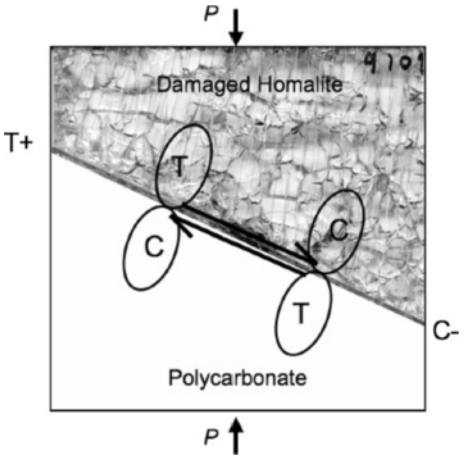

Figure 11

Asymmetries in an undamaged polycarbonate plate in contact with a damaged Homalite plate. Since the polycarbonate is slightly less stiff than the damaged Homalite, the '+' direction of propagation is to the left. The anelastic asymmetry is denoted by the 'C' propagation direction for which the compressional lobe of the crack tip stress concentration travels through the damaged Homalite and the 'T' direction for which the crack tip places the damage in tension. Note that the directions are now 'T+' and 'C−' and are different from the 'C+' and 'T−' directions for Homalite in contact with damaged Homalite in Figure 7.

Table 1

Elastic properties of sample materials

	c_P (m/s)	c_S (m/s)	v
Homalite	2498[(1)]	1200[(1)]	0.35[(1)]
Damaged Homalite	2200[(3)]	1040[(2)]	0.25[(3)]
Polycarbonate	2182[(1)]	960[(1)]	0.38[(1)]

[(1)] Rosakis *et al*. (2008)
[(2)] Biegel *et al*. (2008)
[(3)] O'Connell and Budiansky (1974)

larger angle with the fault plane) and for larger values of v_r/c_S (where v_r is limited to sub-Rayleigh propagation). Note in this figure that all spatial variables are scaled by R_o^*, the length of the slip-weakening zone in the limit of $L \to \infty$ and $v_r \to 0^+$. Note also in Figure 15 that the region of Coulomb failure extends to a distance of about R_o^* at high rupture velocities and when the pre-stress vector is at a large angle to the fault plane.

By fitting their model to Heaton's (1990) estimates of L, δ, and v_r for seven earthquakes, RSP were able to estimate the characteristic displacement δ_1, the dynamic stress drop $(\sigma_{yx}^o - \tau_r)$, the fracture energy G, and R_o^* for each earthquake evaluated at the centroid depth of the rupture (typically about 7 km). Although the seismic parameters estimated by Heaton may be crude, they yield fracture energies that are consistent with

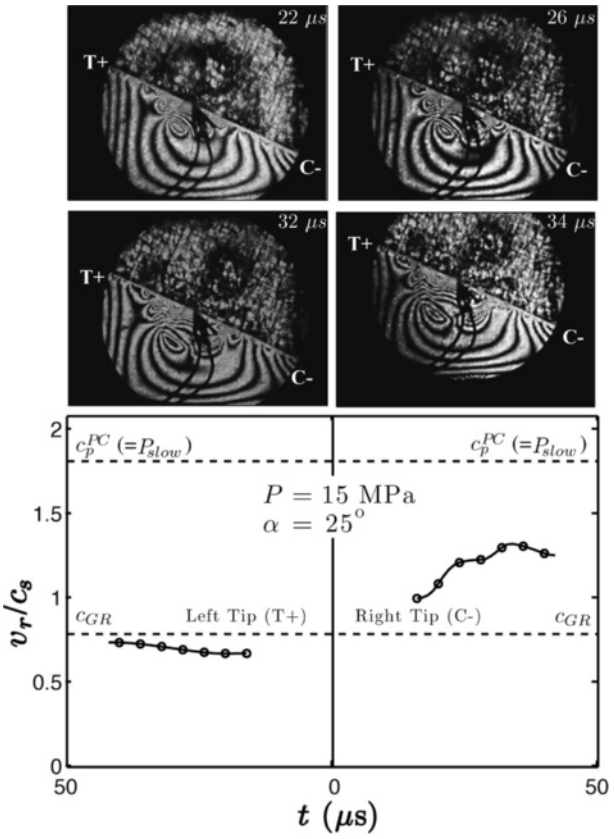

Figure 12
Dynamic rupture on the interface between damaged Homalite and undamaged polycarbonate plates. The upper four panels show frames at the times indicated selected from the sequence of high-speed photographs. The lower panel shows the instantaneous velocity of the rupture tips as a function of time. Note that the left tip propagating in the 'C−' direction transitions to supershear as in Figure 10 but that rupture propagation in the 'T+' direction does not transition to supershear, presumably due to energy loss on the off-fault damage activated by the tensile lobe of the stress field (from Bhat *et al*., 2009).

other estimates both in magnitude and in their dependence on δ (see, e.g., Rice, 2006). RSP found that R_o^* is on the order of 1–40 meters, which is comparable to the width of natural fault zones at seismogenic depth inferred by Li and Malin (2008), It should be noted that the width of natural fault zones at depth is still controversial and may be significantly narrower (Ben-Zion *et al*., 2003; Peng *et al*., 2003; Lewis *et al*., 2005; Finzi *et al*., 2009). On the other hand, the spatial distribution of near-fault seismicity before and after large earthquakes has been interpreted to indicate a damage zone 10–100 meters wide at seismogenic depth (Powers and Jordan, 2009) or even wider (Hauksson, 2009).

We can similarly fit the RSP model to a slip pulse documented by Lu *et al*. (2007) in a Homalite experiment shown in Figure 16. The propagation velocity of the pulse was

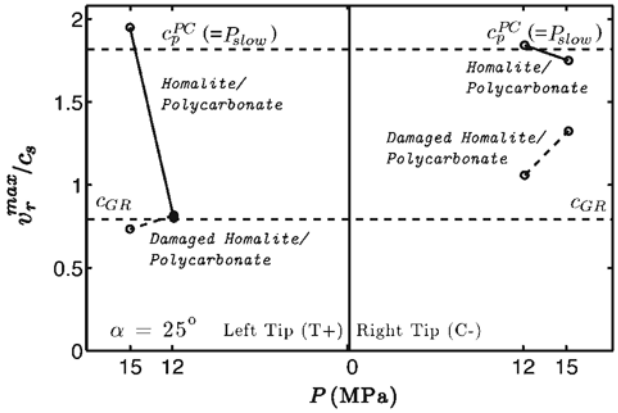

Figure 13
Summary of experimental results comparing rupture velocity in damaged and undamaged bimaterial plates. Note that the off-fault damage has little effect on ruptures traveling in the 'C−' direction but a significant effect on those propagating in the 'T+' direction. Bimaterial ruptures which have the tensile lobe in the damage did not transition to supershear (from BHAT *et al.*, 2009).

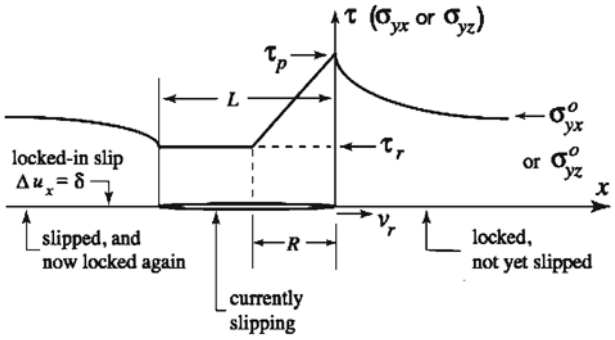

Figure 14
Geometry and parameters of the nonsingular slip-weakening slip-pulse model from RICE *et al.* (2005).

$v_r = 1045$ m/s. Its duration was about 10.2 μs with a rise-time of about 4 μs. This gives $L = 10.7$ mm, $R = 4.2$ mm and, assuming R/L is approximately the ratio of the rise time to the duration, $R/L \sim 0.4$. Integrating the area under the curve gives $\delta = 28$ μm. Since $c_S = 1200$ m/s for Homalite, we have $v_r/c_S = 0.87$. The density of Homalite is 1262 kg/m3 and the shear modulus is $\mu = 1.82$ GPa.

The fracture energy G can be calculated using the graph of $G/\left(\mu\delta^2/\pi L\right)$ vs v_r/c_S with R/L as a parameter given as Figure 15 in RSP. Using the values of v_r/c_S, R/L, μ, δ, and L from the previous paragraph gives $G = 21.2$ J/m^2. It is interesting that $G/\delta \approx 1$ MJ/m^3, close to the value estimated for earthquakes by RICE (2006).

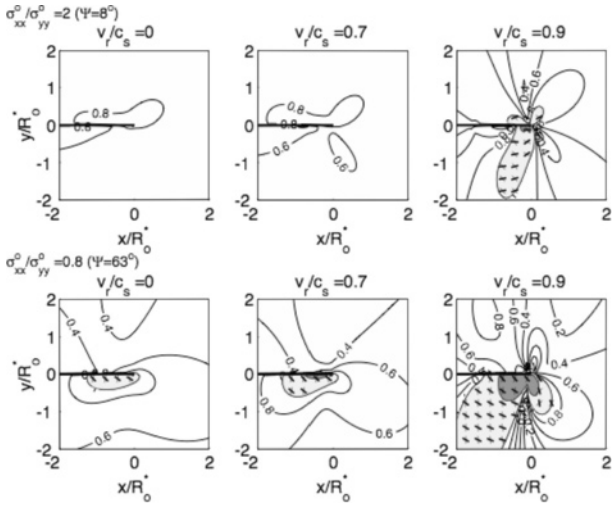

Figure 15

Contour plot of $\tau_{max}/\tau_{Coulomb}$ as a function of position surrounding the tip of a propagating slip pulse when ratio of the weakening distance to the slip length of the pulse is $R/L = 0.1$. Within the shaded areas $\tau_{max}/\sigma_{Coulomb} > 1$ and slip on pre-existing fractures is possible. The short heavy lines within the shaded areas indicate the orientation of optimal planes for right-lateral slip, the short lighter lines for left-lateral slip. The three columns of plots are for different values of the scaled propagation velocity $v_r/c_S = 0$, 0.7 and 0.9. In the top row of plots $\sigma^o_{xx}\big/\sigma^o_{yy} = 2$, in the bottom row $\sigma^o_{xx}\big/\sigma^o_{yy} = 0.8$. All calculations in this figure assume $\tau_r/\tau_p = 0.2$. From RICE *et al.* (2005).

This value of G can then be used to find the dynamic stress drop according to Eq. (15) in RSP: $(\sigma^o_{yx} - \tau_r) = G/\delta = 0.76$ MPa. For the applied uniaxial load of 10 MPa and the fault angle of 20°, the shear and normal stress on the fault plane are $\sigma^o_{yx} = 3.21$ MPa and $\sigma_n = 8.83$ MPa, respectively. The residual stress on the fault plane can be calculated as $\tau_r = \sigma^o_{yx} - (\sigma^o_{yx} - \tau_r) = 2.45$ MPa, which gives a dynamic coefficient of friction of $f_d = \tau_r/\sigma_n = 0.28$. The characteristic slip can then be found as $\delta_1 = \delta(\sigma^o_{yx} - \tau_r)/\left(\tau_p - \tau_r\right) = 7.5$ μm. Finally, the slip-weakening distance can be estimated using Eq. (13) in RSP, where we take $(\tau_p - \tau_r) = \sigma_n(0.6 - 0.28)$

$$R^*_o = \frac{9\pi}{16(1-\nu)}\frac{\mu G}{\left(\tau_p - \tau_r\right)^2} = 11\text{mm}. \quad (1)$$

BIEGEL *et al.* (2008) tested the prediction that the interaction between the crack tip stress field and the damage extends to a distance of about R^*_o. They fabricated a set of samples with a damage band of half width w surrounding the fault plane (Figure 17, left panel) and another set that was totally damaged except for a band of undamaged Homalite of half width w (Fig. 17, right panel). The resultant rupture velocities as a function of w for both damaged and undamaged bands are summarized in Figure 18. Note

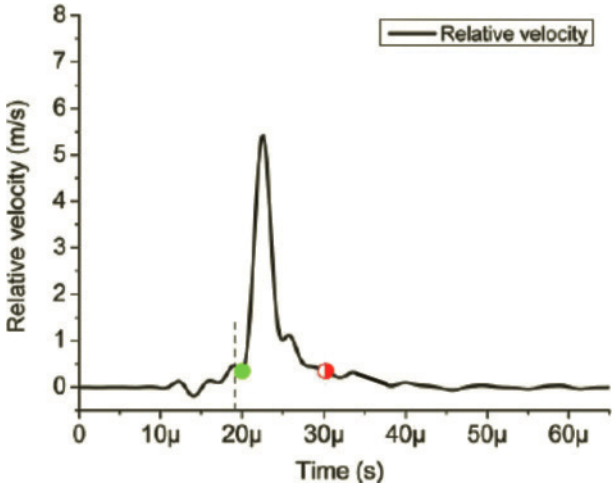

Figure 16
A narrow sub-Rayleigh pulse on the interface between two Homalite plates with $\alpha = 20°$ and $P = 10$ MPa showing the history of relative velocity across the fault plane recorded at 20 mm away from the nucleation point. The dashed line indicates the shear-wave arrival. The solid dot indicates the estimated initiation time of interface sliding. The half-filled dot indicates an estimate of interface locking time (from Lu *et al.*, 2007).

that all rupture velocities were sub-Rayleigh and that most of the change in velocity occurs over a distance $0 < w < 1$ cm, which is about the value of R_o^* estimated above.

6. Discussion

An asymmetric distribution of off-fault damage in a fault zone has been shown to produce strongly directional propagation on the fault plane. The physical source of this directionality is hypothesized to be the interaction between the crack-tip stress field and the off-fault fractures. Ruptures travel more slowly in the 'T' direction for which the tensile lobe of the stress concentration travels through the damage. By comparison, ruptures that travel in the 'C' direction for which the compressive lobe is in the damage propagate as if there were no off-fault damage. Our physical interpretation is that crack-tip compression immobilizes off-fault cracks while crack tip tension enhances frictional slip. It is surprising that the directionality observed in laboratory experiments is so strong (see summaries in Figs. 9 and 13), especially since there was no evidence that new damage was created. The lack of new damage in the experiments is not surprising since the scale-length of the existing damage is about 1 cm—the same size as Ro*. For real earthquakes, Rice *et al.* (2005) estimated Ro* at seismogenic depth to be on the order of meters. Earthquakes should be capable of generating new damage to distances of meters

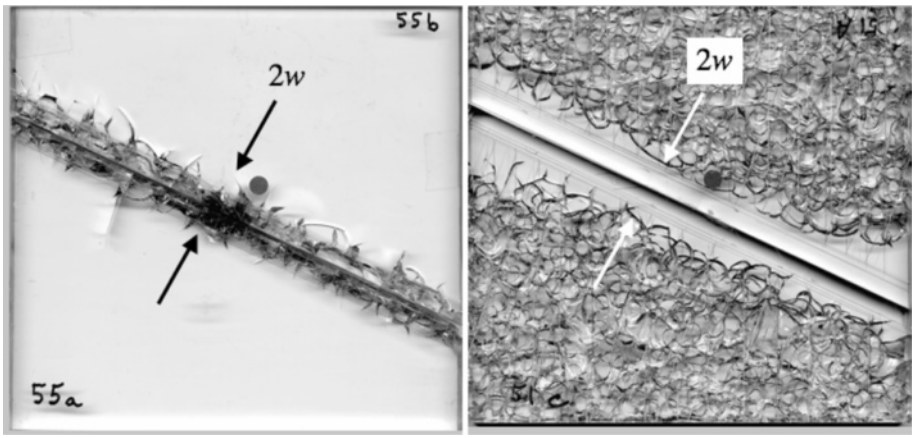

Figure 17
The Homalite plate on the left has a damage band of width $2w$ centered on the fault. The plate on the right has an undamaged band of width $2w$ centered on the fault.

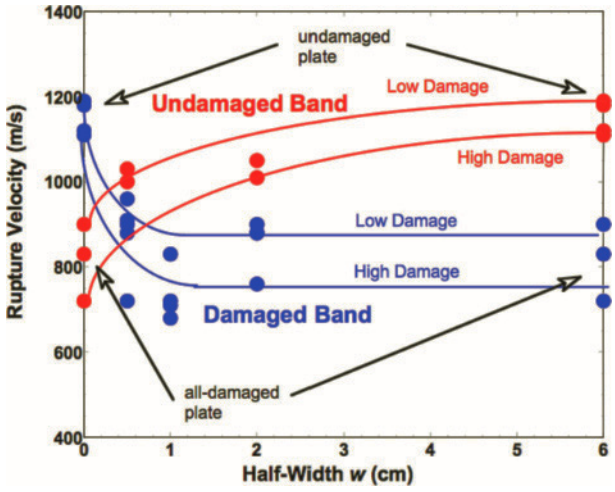

Figure 18
Rupture velocity as a function of w for both damaged and undamaged bands shown in Figure 17. Note that the majority of the decrease in velocity for the damage bands and increase in velocity for the undamaged bands occurs for bands with w less than about 1 cm (from Biegel *et al*., 2008).

from the fault plane, and the generation of new damage is expected to make directional propagation even stronger.

We now return to the central question of how wide a fault zone must be if it is to affect the velocity and symmetry of an earthquake rupture. The simple answer is that the

fault zone must be as wide or wider than *Ro**, the approximate spatial distance to which stress concentration at the rupture tip produces Coulomb slip on the most favorably oriented fractures in the case when the tectonic stress is at a high angle to the fault plane and the rupture velocity is near the Rayleigh limit. Although the preceding analysis used the RICE *et al*. (2005) slip pulse model with slip-weakening friction, other models based on crack-like ruptures and which represent off-fault damage using Coulomb plasticity also find that the nonlinear interaction extends a distance on the order of *Ro** (ANDREWS, 2005; BEN-ZION and SHI, 2005; TEMPLETON and RICE, 2008). The basic difference between slip-pulse and crack-like models is that the spatial extent of the off-fault interaction grows with the propagation of a crack, but reaches a constant value for the slip pulse.

In all these models, the spatial extent of the interaction is also quantitatively related to the ratio of the rupture velocity to the shear-wave speed and the orientation of the remote "tectonic" stress field relative to the fault plane. Additional factors which may affect the interaction between a rupture and off-fault damage but which are not discussed here include the effects of water in the fault zone (see, eg., RICE, 2006), the influence of the nucleation process on the ensuing rupture (SHI and BEN-ZION, 2006; AMPUERO and BEN-ZION, 2008; SHI *et al*., 2008), and the case of supershear rupture. The experimental results reviewed here found that off-fault damage suppresses supershear propagation in all cases in which the tensile lobe of the rupture tip stress field encounters off-fault damage. This may be one reason why supershear earthquake ruptures are relatively rare.

Acknowledgements

The authors wish to thank Yehuda Ben-Zion and an anonymous reviewer for many helpful suggestions. The authors acknowledge support of the National Science Foundation collaborative grant EAR-0711171 to the University of Southern California and the California Institute of Technology. This research was supported by the Southern California Earthquake Center. SCEC is funded by NSF Cooperative Agreement EAR-0106924 and USGS Cooperative Agreement 02HQAG0008. The SCEC contribution number for this paper is 1227.

REFERENCES

AMPUERO, J.-P. and BEN-ZION, Y. (2008), *Cracks, pulses and macroscopic asymmetry of dynamic rupture on a bimaterial interface with velocity-weakening friction*, Geophys. J. Int. *173*, 674–692, doi: 10.1111/j.1365-246X.2008.03736.x.

ANDREWS, D.J. (2005), *Rupture dynamics with energy loss outside the slip zone*, J. Geophys. Res. *110*, B01307, doi:10.1029/2004JB003191.

BEN-ZION, Y. (2001), *Dynamic ruptures in recent models of earthquake faults*, J. Mech. Phys. Sol. *49*, 2209–2244.

BEN-ZION, Y. and SAMMIS, C.G. (2003), *Characterization of Fault Zones*, Pure Appl. Geophys. *160*(3), 677–715.

BEN-ZION, Y. and SHI, Z. (2005), *Dynamic rupture on a material interface with spontaneous generation of plastic strain in the bulk*, Earth Planet. Sci. Lett. *236*, 486–496, DOI, 10.1016/j.epsl.2005.03.025.

BEN-ZION, Y., PENG, Z., OKAYA, D., SEEBER, L., ARMBRUSTER, J.G., OZER, N., MICHAEL, A.J., BARIS, S., and AKTAR, M. (2003), *A shallow fault zone structure illuminated by trapped waves in the Karadere-Duzce branch of the North Anatolian Fault, western Turkey*, Geophys. J. Int. *152*, 699–717.

BHAT, H.S., BIEGEL, R.L., ROSAKIS, A.J., and SAMMIS, C.G. (2009), *The effect of asymmetric damage on dynamic shear rupture propagation II: With mismatch in bulk elasticity*, J. Geophs. Res., in press.

BIEGEL, R.L. and SAMMIS, C.G. (2004), *Relating fault mechanics to fault zone structure*, Adv. Geophys. *47*, 65–111.

BIEGEL, R.L., SAMMIS, C.G., and ROSAKIS, A.J. (2008), *An experimental study of the effect of off-fault damage on the velocity of a slip pulse*, J. Geophys. Res. *113*, B04302, doi:10.1029/2007JB005234.

BIEGEL, R.L., BHAT, H.S., SAMMIS, C.G., and ROSAKIS, A.J. (2009), *The effect of asymmetric damage on dynamic shear rupture propagation I: No mismatch in bulk elasticity*, J. Geophys. Res., in press.

COCHARD, A. and RICE, J.R. (2000), *Fault rupture between dissimilar materials- Ill-posedness, regularization, and slip-pulse response*, J. Geophy. Res. *105* (B11), 25,891–25,907.

DOR, O., BEN-ZION, Y., ROCKWELL, T.K., and BRUNE, J. (2006), *Pulverized rocks in the Mojave section of the San Andreas Fault Zone*, Earth Planet. Sci. Lett. *245*, 642–654.

FINZI, Y., HEARN, E.H., BEN-ZION, Y., and LYAKHOVSKY, V. (2009), *Structural properties and deformation patterns of evolving strike-slip faults: Numerical simulations incorporating damage rheology*, Pure Appl. Geophys., in press.

HARRIS, R.A. and DAY, S.M. (1997), *Effects of a low-velocity zone on a dynamic rupture*, Bull. Seismol. Soc. Am. *87*(5), 1267–1280.

HAUKSSON, E. (2008), *Spatial separation of large earthquakes, aftershocks, and background seismicity: Analyisi of interseismic and coseismic seismicity patterns in southern California*, Pure Appl. Geophys., in press.

HEATON, T.H. (1990), *Evidence for and implications of self-healing pulses of slip in earthquake rupture*, Phys. Earth Planet. Int. *64*(1), 1–20.

LEWIS, M.A., PENG, Z., BEN-ZION, Y., and VERNON, F. (2005), *Shallow seismic trapping structure in the San Jacinto fault zone*, Geophys. J. Int. *162*, 867–881, doi:10.1111/j.1365-246X.2005.02684.x.

LI, Y.G. and MALIN, P.E. (2008), *San Andreas Fault damage at SAFOD viewed with fault-guided waves*, Geophys. Res. Lett. *35*(8), L08304, doi:10.1029/2007GL032924.

LU, X., LAPUSTA, N., and ROSAKIS, A.J. (2007), *Pulse-like and crack-like ruptures in experiments mimicking crustal earthquakes*, Proc. Natl. Acad. Sci. USA *104*(48), 18,931–18,936, doi:10.1073/pnas.0704268104.

O'CONNELL, R.J. and BUDIANSKY, B. (1974), *Seismic velocities in dry and saturated cracked solids*, J. Geophys. Res. *79*(35), 5412–5426.

PENG, Z., BEN-ZION, Y., MICHAEL, A.J., and ZHU, L. (2003), *Quantitative analysis of seismic trapped waves in the rupture zone of the 1992 Landers, California earthquake: Evidence for a shallow trapping structure*, Geophys. J. Int. *155*, 1021–1041.

POWERS, P.M. and JORDAN, T.H. (2009), *Distribution of seismicity across strike-slip faults in California*, J. Geophys. Res., in press.

RANJITH, K. and RICE, J.R. (2001), *Slip dynamics at an interface between dissimilar materials*, J. Mech. Phys. Solids *49*, 341–361.

RICE, J.R. (2006), *Heating and weakening of faults during earthquake slip*, J. Geophys. Res. *111*, B05311, doi:10.1029/2005JB004006,

RICE, J.R., SAMMIS, C.G., and PARSONS, R. (2005), *Off-fault secondary failure induced by a dynamic slip pulse*, Bull. Seismol. Soc. Amer. *95*(1), 109–134.

ROSAKIS, A.J., XIA, K., LYKOTRATIS, G., and KANAMORI, H. (2008), *Dynamic shear rupture in frictional interfaces: Speeds, Directionality and Modes*. In *Treatise in Geophysics* (ed. H. KANAMORI), Vol. 4, 153–192.

RUBIN, A.M. and AMPUERO, J.-P. (2007), *Aftershock asymmetry on a bimaterial interface*, J. Geophys. Res. *112*, B05307, doi:10.1029/2006JB004337.

SHI, Z.Q. and BEN-ZION, Y. (2006), *Dynamic rupture on a bimaterial interface governed by slip-weakening friction*, Geophys. J. Int. *165*, 469–484.

SHI, Z.Q., BEN-ZION, Y., and NEEDLEMAN, A. (2008), *Properties of dynamic rupture and energy partition in a two-dimensional elastic solid with a frictional interface*, J. Mech. Phys. Solids *56*, 5–24, doi:10.1016/j.jmps.2007.04.006.

TEMPLETON, E.L. and RICE, J.R. (2008), *Off-fault plasticity and earthquake rupture dynamics, 1. Dry materials or neglect of fluid pressure changes*, J. Geophys. Res. *113*, B09306, doi:10.1029/2007JB005529.

WEERTMAN, J. (1980), *Unstable slippage across a fault that separates elastic media of different elastic constants*, J. Geophys. Res. *85*, 1455–1461.

XIA, K., ROSAKIS, A.J., and KANAMORI, H. (2005a), *Supershear and sub-Rayleigh to supershear transition observed in laboratory earthquake experiments*, Exp. Tech. *29*, 63–66.

XIA, K., ROSAKIS, A.J., KANAMORI, H., and RICE, J.R. (2005b), *Laboratory earthquakes along inhomogeneous faults: Directionality and supershear*, Science *308*, 681–684.

(Received October 6, 2008, accepted March 23, 2009)
Published Online First: July 29, 2009